

Topologically Ordered Amorphous Silica Obtained from the Collapsed Siliceous Zeolite, Silicalite-1-F: A Step toward “Perfect” Glasses

Julien Haines,^{*,†} Claire Levelut,[‡] Aude Isambert,[§] Philippe Hébert,[§] Shinji Kohara,^{||}
David A. Keen,^{⊥,#} Tahar Hammouda,[∇] and Denis Andraud[∇]

Institut Charles Gerhardt Montpellier, Equipe PMOF, UMR 5253 CNRS-UM2-ENSCM-UM1, Université Montpellier II, Sciences et Techniques du Languedoc, Place E. Bataillon cc1504, 34095 Montpellier Cedex 05, France, Laboratoire des Colloïdes, Verres et Nanomatériaux, UMR 5587 CNRS UM2, Université Montpellier II, Place Eugène Bataillon, 34095 Montpellier Cedex 5, France, CEA, DAM Le Ripault, F-37260 Monts, France, Research & Utilization Division, Japan Synchrotron Radiation Research Institute (JASRI, SPring-8) I-1-1 Kouto, Sayo-cho, Sayo-gun, Hyogo 679-5198, Japan, ISIS Facility, Rutherford Appleton Laboratory, HSIC, Didcot, Oxfordshire, OX11 0QX, United Kingdom, Department of Physics, Oxford University, Clarendon Laboratory, Parks Road, Oxford, OX1 3PU, United Kingdom, Laboratoire Magmas et Volcans, UMR CNRS 6524, Université Blaise Pascal, 63038 Clermont-Ferrand Cedex, France

Received May 19, 2009; E-mail: jhaines@lpmc.univ-montp2.fr

Abstract: A dense amorphous form of silica was prepared at high pressure from the highly compressible, siliceous zeolite, silicalite-1-F. Reverse Monte Carlo modeling of total X-ray scattering data shows that the structure of this novel amorphous form of SiO₂ recovered under ambient conditions is distinct from vitreous SiO₂ and retains the basic framework topology (i.e., chemical bonds) of the starting crystalline zeolite. This material is, however, amorphous over the different length scales probed by Raman and X-ray scattering due to strong geometrical distortions. This is thus an example of new topologically ordered, amorphous material with a different intermediate-range structure, a lower entropy with respect to a standard glass, and distinct physical and mechanical properties, eventually approaching those of an “ordered” or “perfect” glass. The same process in more complex aluminosilicate zeolites will, in addition, lead to an amorphous material which conserves the framework topology and chemical order of the crystal. The large volume collapse in this material may also be of considerable interest for new applications in shock wave absorption.

Introduction

Glasses are used for a large number of technological and everyday applications. One principal drawback of glasses is their fragility. The existence of polymorphism in liquids and glasses,^{1,2} transitions between low- and high-density liquid or glassy forms, and the resulting modifications to physical properties has stimulated a great deal of interest in the nature of densified silica glass^{3–13} with respect to standard glass. In particular, this “polyamorphism” gives rise to amorphous materials with the

same chemical composition, but with different densities and entropies. This is of interest with respect to Kauzmann’s paradox;¹⁴ that is the extrapolated entropy of a liquid at low temperature is lower than that of the low-temperature crystalline phase. The glass transition intervenes on cooling prior to the formation of a low-entropy amorphous material or “perfect glass”¹⁵ (i.e., structural order close to that of the crystal), which can be expected to have improved mechanical properties (lower fragility) with respect to standard glass.

- [†] Institut Charles Gerhardt Montpellier, Université Montpellier II.
[‡] Laboratoire des Colloïdes, Verres et Nanomatériaux, Université Montpellier II.
[§] CEA, DAM Le Ripault.
^{||} JASRI, SPring-8.
[⊥] Rutherford Appleton Laboratory.
[#] Oxford University.
[∇] Laboratoire Magmas et Volcans, Université Blaise Pascal.
- (1) Brazhkin, V. V.; Lyapin, A. G. *J. Phys.: Condens. Matter* **2003**, *15*, 6059–6084.
 - (2) McMillan, P. F.; Wilson, M.; Wilding, M. C.; Daisenberger, D.; Mezouar, M.; Greaves, G. N. *J. Phys.: Condens. Matter* **2007**, *19*, 415101–415141.
 - (3) McMillan, P.; Piriou, B.; Couty, R. *J. Chem. Phys.* **1984**, *81*, 4234–4236.
 - (4) Hemley, R. J.; Mao, H. K.; Bell, P. M.; Mysen, B. O. *Phys. Rev. Lett.* **1986**, *57*, 747–750.

- (5) Walrafen, G. E.; Chu, Y. C.; Hokmabadi, M. S. *J. Chem. Phys.* **1990**, *92*, 6987–7002.
- (6) Susman, S.; Volin, K. J.; Price, D. L.; Grimsditch, M.; Rino, J. P.; Kalia, R. K.; Vashishta, P. *Phys. Rev. B* **1991**, *43*, 1194–1197.
- (7) Meade, C.; Hemley, R. J.; Mao, H. K. *Phys. Rev. Lett.* **1992**, *69*, 1387–1390.
- (8) Sugai, S.; Sotokawa, H.; Kyokane, D.; Onodera, A. *Phys. B* **1996**, *219–220*, 293–295.
- (9) Sugai, S.; Onodera, A. *Phys. Rev. Lett.* **1996**, *77*, 4210–4213.
- (10) Inamura, Y.; Arai, M.; Kitamura, N.; Bennington, S. M.; Hannon, A. C. *Phys. B* **1998**, *241–243*, 903–905.
- (11) Inamura, Y.; Katayama, Y.; Utsumi, W.; Funakoshi, K. *Phys. Rev. Lett.* **2004**, *93*, 015501–4.
- (12) Katayama, Y.; Inamura, Y. *Nucl. Instrum. Methods.* **2005**, *B238*, 154–159.
- (13) Sato, T.; Funamori, N. *Phys. Rev. Lett.* **2008**, *101*, 255502–4.
- (14) Kauzmann, W. *Chem. Rev.* **1948**, *43*, 219–256.
- (15) Greaves, G. N.; Sen, S. *Adv. Phys.* **2007**, *56*, 1–166.

Another method of preparing novel amorphous forms is by pressure-induced amorphization (PIA) of crystalline phases.^{16,17} PIA can yield distinct amorphous forms with important structural differences with respect to quenched liquids or densified glasses. This can thus help to better understand the processes of temperature-induced vitrification, pressure-induced densification and PIA. The investigation of the different amorphous forms of silica and related materials can improve our understanding of the physics and chemistry of glasses and liquids and enable the design of new amorphous materials with original properties.

PIA of open-structured, microporous materials such as zeolites^{18–30} provides another route to prepare distinct amorphous solids. These microporous materials, if compressed slowly enough, were predicted to potentially tend toward the state of a “perfect” glass by Greaves et al.^{15,24,25} Zeolites are low-density, porous aluminosilicates built up of corner-sharing SiO₄ and AlO₄ tetrahedra and are extensively used in important technological applications as molecular sieves and catalysts.^{31–34} PIA is also of interest in these materials as the origin of a new potential application of zeolites—related to their high porosity—as shock wave absorbers in the field of energetic materials safety.²⁹ In the prototypic zeolite faujasite, for example, PIA is accompanied by local depressurization effects due to the amorphization of the crystalline phase and an increase in density of the amorphous form at the LDA (low density amorphous)—HDA (high density amorphous) transformation.^{24,25,28,29} Such local decompression effects provide a key mechanism for shock wave absorption in this material. Clearly, in order to understand local depressurization better, it is important to have structural information on the high-pressure amorphous forms. A key point is also to determine if there is any remaining structural order in these amorphous forms and whether they tend toward “perfect” glasses. The present work focuses on the preparation of a novel

dense amorphous form of SiO₂ obtained from the structural collapse of the zeolite silicalite-1-F upon compression at room temperature.

Experimental Section

Calcined silicalite-1-F was obtained from SOMEZ (France). This material is essentially pure SiO₂ and was prepared by the fluoride route,^{35,36} using tetrapropylammonium cations as a templating agent, followed by calcination. This method yields a product with 0.9% fluorine before calcination, but this value will have significantly decreased in the final sample.

Angle-dispersive X-ray diffraction data at high pressure were obtained using a diamond anvil cell (DAC). The starting material was monoclinic, space group *P2₁/n* with cell parameters *a* = 19.8933(3) Å, *b* = 20.1227(3) Å, *c* = 13.3746(3) Å, and *β* = 90.657(2)° with a density of 1.787 g/cm³. The silicalite-1-F sample was placed in the 140 μm hole of a tungsten gasket preindented to 100 μm. NaCl was added as pressure calibrant and as an intensity reference. Runs were performed with and without silicone oil, a nonpenetrating pressure-transmitting medium that does not enter the pores of the silicalite structure. Two-dimensional, X-ray diffraction patterns were obtained on an imaging plate using zirconium-filtered, molybdenum radiation from a microfocus tube. The sample to imaging plate distance was 143.69 mm. Acquisition times were of the order of 48–60 h. Pressures were measured based on the equation of state of NaCl.³⁷ Cell parameters were obtained by full-profile fitting using the program Fullprof.³⁸ The pressure-volume data were fitted using a second-order Birch–Murnaghan equation of state.³⁹ This second-order expansion fixes the first derivative of the bulk modulus to 4. An additional exposure on the starting mixture of silicalite-1-F and NaCl in a 0.3 mm X-ray capillary was performed on the same diffractometer.

A Walker-type multianvil apparatus was used to prepare the amorphous silicalite-1-F following the previously described procedure.⁴⁰ A total of 9.45 mg of powdered sample was placed in a 2.7 mm long, 2.5 mm internal diameter gold capsule and was loaded in a 10 mm edge length MgO octahedral sample cell. The sample cell was placed between the eight tungsten carbide anvils cubes with 32 mm edge lengths and a truncated face of 5 mm edge length in contact with the octahedron. Preformed 5 × 2 mm gaskets were used. This assembly was then positioned between the outer six anvils of the 1000 tonne, split-cylinder, multianvil device. The pressure was increased to 20 GPa over a period of 3.5 h and held at this pressure for 1 h. The sample was decompressed slowly over a period of 15 h.

Raman spectra were obtained using a Horiba Jobin-Yvon Labram Aramis spectrometer. The samples were placed under the 50× or 100× objectives of the Olympus microscope. 473 nm (silicalite-1-F and silica glass) and 785 nm (pressure-amorphized silicalite-1-F) diode lasers were used for excitation with edge filter cutoffs beginning at 105 and 75 cm⁻¹, respectively.

High energy X-ray diffraction data from the recovered amorphous sample were obtained using the two axis diffractometer and 61.6 keV X-rays on the beamline BL04B2 at SPring-8. The details of experiment and standard data analysis are described elsewhere.^{41,42}

(16) Sharma, S. M.; Sikka, S. K. *Prog. Mater. Sci.* **1996**, *40*, 1–77.

(17) Richet, P.; Gillet, P. *Eur. J. Mineral.* **1997**, *9*, 907–933.

(18) Gillet, P.; Malézieux, J. M.; Itié, J. P. *Am. Mineral.* **1996**, *81*, 651–657.

(19) Huang, Y. *J. Mater. Chem.* **1998**, *8*, 1067–1071.

(20) Rutter, M. D.; Uchida, T.; Secco, R. A.; Huang, Y.; Wang, Y. *J. Phys. Chem. Solids* **2001**, *62*, 599–606.

(21) Liu, H.; Secco, R. A.; Huang, Y. *PhysChemComm* **2001**, *8*, 1–3.

(22) Comodi, P.; Gatta, G. D.; Zanazzi, P. F. *Eur. J. Mineral.* **2001**, *13*, 497–505.

(23) Havenga, E. A.; Huang, Y.; Secco, R. A. *Mater. Res. Bull.* **2003**, *38*, 381–387.

(24) Greaves, G. N.; Meneau, F.; Sapelkin, A.; Gwynn, I.; Wade, S.; Sankar, G. *Nat. Mater.* **2003**, *2*, 622–629.

(25) Greaves, G. N.; Meneau, F. *J. Phys.: Condens. Matter* **2004**, *16*, S3459–S3472.

(26) Colligan, M.; Forster, P. M.; Cheetham, A. K.; Lee, Y.; Vogt, T.; Hriljac, J. A. *J. Am. Chem. Soc.* **2004**, *126*, 12015–12022.

(27) Peral, I.; Ñíguez, J. *Phys. Rev. Lett.* **2006**, *97*, 225502–4.

(28) Greaves, G. N.; Meneau, F.; Kargl, F.; Ward, D.; Holliman, P.; Albergamo, F. *J. Phys.: Condens. Matter* **2007**, *19*, 415102–17.

(29) Isambert, A.; Angot, E.; Hébert, P.; Haines, J.; Levelut, C.; Le Parc, R.; Ohishi, Y.; Kohara, S.; Keen, D. A. *J. Mater. Chem.* **2008**, *18*, 5746–5752.

(30) Readman, J. E.; Forster, P. M.; Chapman, K. W.; Chupas, P. J.; Parise, J. B.; Hriljac, J. A. *Chem. Commun.* **2009**, 3383–3385.

(31) Breck, D. W. *Zeolite Molecular Sieves: Structure, Chemistry and Use*; Wiley: New York, 1974.

(32) Galarneau, A.; Di Renzo, F.; Fajula, F.; Vadrine, J. *Zeolites and Mesoporous at the Dawn of the 21st Century*; Elsevier: Amsterdam, 2001.

(33) Auerbach, S. M.; Carrado, K. A.; Dutta, P. K. *Handbook of Zeolite Science and Technology*; Marcel Dekker, Inc.: New York/Basel, 2003.

(34) Bish, D. L.; Ming, D. W. *Rev. Miner. Geochem.* **2001**, *45*, 1–654.

(35) Guth, J. L.; Kessler, H.; Rey, R. In *Proceedings of the 7th International Zeolite Conference*; Murakami, Y., Lilima, A.; Ward, J. W., Eds.; Kodansha/Elsevier: Tokyo, 1986; p 121.

(36) Brémard, C.; Laureys, J.; Patarin, J. *J. Raman Spectrosc.* **1996**, *27*, 439–445.

(37) Birch, F. *J. Geophys. Res.* **1986**, *91*, 4949–4954.

(38) Rodriguez-Carvajal, J. *Comm. Powder Diffr. Newsletter* **2001**, *26*, 12–19.

(39) Birch, F. *Phys. Rev.* **1947**, *71*, 809–824.

(40) Hammouda, T. *Earth Planet. Sci. Lett.* **2003**, *214*, 357–368.

(41) Isshiki, M.; Ohishi, Y.; Goto, S.; Takeshita, K.; Ishikawa, T. *Nucl. Instrum. Methods* **2001**, *A467–468*, 663–666.

(42) Kohara, S.; Itou, M.; Suzuya, K.; Inamura, Y.; Sakurai, Y.; Ohishi, Y.; Takata, M. *J. Phys.: Condens. Matter* **2007**, *19*, 506101–506115.

The density of the amorphous form was estimated with an accuracy of $\pm 5\%$ on the basis of the X-ray pair distribution function to be $0.08119 \text{ atoms}/\text{\AA}^3$ ($2.7 \text{ g}/\text{cm}^3$).

The starting RMC model was obtained by progressively reducing the volume of a $2 \times 2 \times 4$ orthorhombic supercell of the silicalite structure while randomly moving atoms to maintain local tetrahedral geometry and network topology. Once the model had attained the measured pressure amorphized sample density (model size $35.344 \times 34.726 \times 46.244 \text{ \AA}^3$), the model was further refined using RMC protocols⁴³ by minimizing the difference between the $S(Q)$ calculated from the model and the experimental $S(Q)$ while retaining a weaker restraint on the tetrahedral geometry.⁴⁴ Although the starting network topology is implicitly maintained by these geometric restraints, further bonding between atoms is not prevented. Attempts to improve the model using RMC by imposing less constraints still (i.e., only restraining coordination and shortest distances pairs of atoms may approach and not maintaining silicalite topology) produced a less physically sensible model and a poorer fit to the data. This gives further credibility to the model structure reported here. There are, however, some minor limitations in the resulting model, largely due to the small size of the model and the isotropic densification method. For example, the deformed pores in the amorphous model are still approximately linear. Effects relating to (e.g.) shear forces would not necessarily be introduced in the structure and consequently buckling of the pore channels is unlikely to take place to any great extent.

Results and Discussion

Pressure-Induced Amorphization of Silicalite-1-F. Calcined, hydrophobic silicalite-1-F was studied at high pressure by angle-dispersive X-ray diffraction using both a nonpenetrating pressure-transmitting medium (silicone oil) and without a medium. In both cases, the intensities of the diffraction lines of silicalite-1-F were found to decrease immediately on pressure increase, Figure 1A. With the use of silicone oil as a pressure-transmitting medium (PTM), a very strong decrease in intensity occurs just above 3 GPa with complete disappearance of the diffraction lines just above 8.6 GPa. In the absence of a PTM, the decrease in intensity is more gradual with complete disappearance occurring above 14.6 GPa.

Silicalite-1-F is highly compressible, Figure 1B. The bulk modulus over the low pressure range in silicone oil is $13.6(5) \text{ GPa}$, three times more compressible than faujasite²⁹ or quartz.⁴⁵ Above 3 GPa, the remaining crystalline phase exhibits a bulk modulus of $9.98(9) \text{ GPa}$. The behavior in the absence of a PTM is very different. Above 3 GPa, the apparent relative volume is 5–10% higher than in silicone oil and a very strong apparent volume increase is observed above 10 GPa. Such apparent volume increases under pressure have been reported previously for zeolite A^{24,25,28} and faujasite²⁹ and linked to local depressurization effects in mixtures of remaining crystalline material and amorphous forms of different densities. Effectively, in this complex microstructure, local decompression within the powder grains results in a lower pressure being experienced by the remaining crystalline phase in the amorphous matrix with respect to the NaCl pressure marker. This is clearly nonequilibrium behavior. Such local depressurization can also explain the

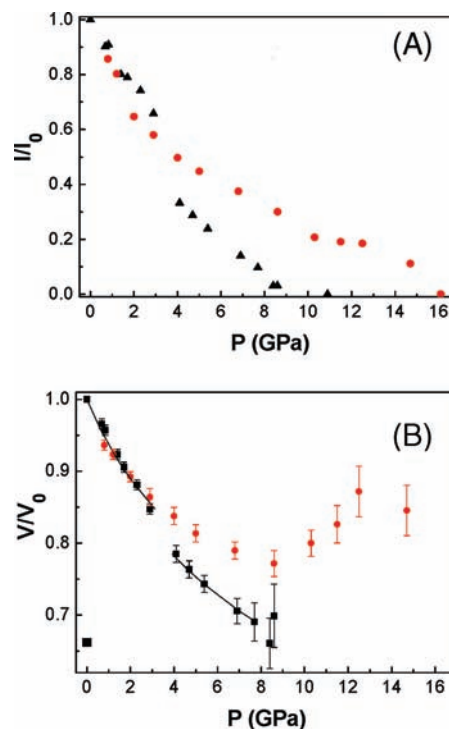


Figure 1. Relative intensity of the strongest diffraction line initially at $2\theta = 3.65^\circ$ ($d = 11.159 \text{ \AA}$) (A) and relative volume (B) of silicalite-1-F in silicone oil (triangles, small squares) and without a PTM (●) as a function of pressure. The large square (■) indicates the relative volume of RMC model of the recovered amorphous form. Solid lines represent fits to the data using a Birch–Murnaghan equation of state.³⁹

persistence of the crystalline phase to much higher pressure in the absence of a PTM. These results can explain the potential shock wave absorption properties of this material, as this local decompression also partially “absorbs” the applied static pressure. These effects are particularly marked in silicalite-1-F, for which the pores are empty, as compared to hydrated aluminosilicate zeolites such as zeolite A^{24,25,28} and faujasite.²⁹

High-Pressure Synthesis, Vibrational and Structural Study of Amorphous Silicalite-1-F. To understand the process better, to directly study the structure of the amorphous form of silicalite-1-F, and to compare it with the initial silicalite structure, a millimeter-sized sample was prepared and recovered from 20 GPa at room temperature using a multianvil high-pressure device. The recovered material was transparent and glass-like in appearance. The Raman spectrum of the recovered sample, Figure 2, is very different from that of the initial silicalite phase and from that of silica glass. It exhibits strong bands typical for amorphous silica at 510 and 618 cm^{-1} along with weaker features near 798 , 847 , 994 , and 1224 cm^{-1} . A shoulder is observed at 451 cm^{-1} and the Bose peak at close to 90 cm^{-1} . The strong bands lie close to those of the D_1 and D_2 defect bands of silica glass, which have been linked to the presence of four-membered and three-membered rings (MR) of SiO_4 tetrahedra, respectively.⁴⁶ This region of the spectrum resembles that of permanently densified silica glass,^{3,4,8} which may be linked to a shift in ring statistics with respect to silicalite-1-F, leading to the formation of 3 MRs and 4 MRs; silicalite-1-F is characterized by the presence of 4, 5, 6, and 10 MRs. Another possibility is the presence of highly strained O–Si–O and

(43) Tucker, M. G.; Keen, D. A.; Dove, M. T.; Goodwin, A. L.; Hui, Q. *J. Phys.: Condens. Matter* **2007**, *19*, 335218–335216.

(44) This was achieved using a combination of ‘distance window’ constraints on Si–O, O–O and Si–Si distances and polyhedral restraints on the Si–O bond length and O–Si–O bond angles within the program RMCProfile.⁴³ After densification, the distance window constraints were removed but the polyhedral restraints were retained.

(45) Angel, R. J.; Allan, D. R.; Miletich, R.; Finger, L. W. *J. Appl. Crystallogr.* **1997**, *30*, 461–466.

(46) Galeener, F. L.; Barrio, R. A.; Martinez, E.; Elliot, R. J. *Phys. Rev. Lett.* **1984**, *53*, 2429–2432.

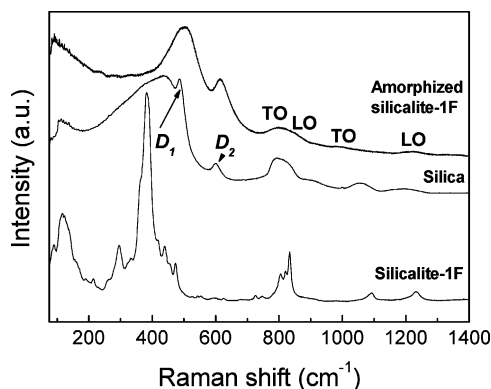


Figure 2. Raman spectra of silicalite-1-F, silica glass and pressure amorphized silicalite-1-F.

Si–O–Si angles in the collapsed silicalite structure. A notable difference between amorphized silicalite and silica glass (normal and densified) is visible in the two weak, highest frequency modes corresponding to the LO (1224 cm^{-1}) and TO (994 cm^{-1}) antisymmetric Si–O–Si stretching modes.⁴⁷ In the present case, the TO – LO splitting is significantly greater, which would be consistent with an increase in polar character. In addition, the TO (798 cm^{-1}) – LO (847 cm^{-1}) splitting of the partially resolved, symmetric Si–O–Si stretching mode near 800 cm^{-1} is more than twice that observed for silica glass. The TO – LO splitting in silica glass was found to arise from strong coupling between the optic modes and low-frequency shear and stress waves.⁵

Total X-ray scattering data, Figure 3A, were obtained on the two-axis diffractometer at the beamline BL04B2 at SPring-8^{41,42} and correspond to a characteristic broad pattern of an amorphous material. The first sharp diffraction peak (FSDP) of the pressure amorphized silicalite-1-F lies at close to 1.82 \AA^{-1} , which is much greater than that of silica glass,¹⁰ 1.53 \AA^{-1} . A strong increase in the FSDP position has been observed as functions of pressure and density in previous studies and has been related to changes in the intermediate-range order in these systems.^{6,7,9–11} The value for pressure amorphized silicalite-1-F is significantly higher than glass densified at room temperature and slightly higher than that densified under pressure at high temperature. In addition, as in densified silica glass, the second peak at about 4.8 \AA^{-1} is very intense and different from normal silica glass.

Reverse Monte Carlo (RMC) modeling was used to determine the structure of amorphous silicalite-1-F. A very good fit was obtained to $S(Q)$, Figure 3A, and the resulting model is compared to silicalite-1-F and silica glass⁴⁸ in Figure 4. Significantly, the model $S(Q)$ shows no Bragg peaks (Figure 3A) with no long-range oscillations in the partial radial distribution functions, $g_{ij}(r)$, (Figure 3B), showing that the model is truly amorphous, despite originating from the low-pressure crystal structure. On the basis of the total correlation functions $T(r)$ (Figure 5), the Si–O bond length of 1.62 \AA is only slightly greater than that of normal silica glass.⁴⁸ In the partial radial distribution functions ($g_{ij}(r)$), Figure 3B, the O–O and Si–Si distributions in amorphous silicalite-1-F are much broader, an indication of a wider distribution of O–Si–O and Si–O–Si angles in amorphous silicalite-1-F as compared to silica glass. The Si–Si peak is at a shorter distance in amorphous silicalite-

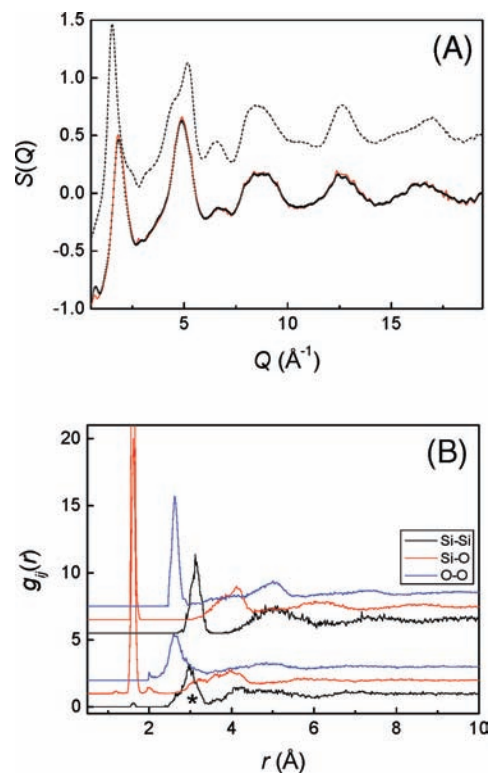


Figure 3. (A) X-ray total structure factor $S(Q)$ of pressure-amorphized silicalite-1-F (+) and calculated $S(Q)$ from the RMC refined model (red solid line). $S(Q)$ data for silica glass (dashed line) are shifted vertically for clarity. (B) Partial radial distribution functions from the RMC model of pressure-amorphized silicalite-1-F and silica glass⁴⁸ (lower and upper traces, respectively; traces are also shifted vertically for clarity). Note the double peak in the Si–Si distribution in pressure-amorphized silicalite-1-F near 3 \AA (*).

1-F (just less than 3 \AA rather than about 3.1 \AA). There are differences in the intertetrahedral Si–O distributions reflecting significant distortions of the different rings. Note also that pair distribution function data for densified silica⁶ bear a greater resemblance to normal silica glass than pressure-amorphized silicalite-1-F.

It is interesting to compare the results on pressure-amorphized silicalite-1-F with those of the amorphous precursor and the crystalline phase of the silica-rich zeolite ZSM-5,⁴⁹ which has the same structure as silicalite-1-F. The PDF of the amorphous zeolite precursor is quite similar to that of normal silica glass and very different from pressure-amorphized silicalite-1-F. The PDF of the crystalline phase is very similar to that of silica glass up to 4.5 \AA , but very different for larger distances. The PDF of pressure-amorphized silicalite-1-F (Figure 5) presents a much greater number of discrete peaks and shoulders rather than smoothly varying broad features. This indicates a smaller number of distinct distance distributions that arise from a smaller number of characteristic structural motifs. However, the collapse of the pores of the zeolite structure introduces further close contacts such that (for example) intertetrahedral Si–O distributions linked to 4 (3.5 \AA , 3.8 \AA), 5 (3.7 \AA , 3.9 \AA , 4.0 \AA , 4.2 \AA) and 6 (3.5 \AA , 3.9 \AA , 4.0 \AA , 4.2 \AA) MRs are particularly predominant for all systems. The present results indicate that

(47) Galeener, F. L.; Lucovsky, G. *Phys. Rev. Lett.* **1976**, *37*, 1474–1478.

(48) Tucker, M. G.; Keen, D. A.; Dove, M. T.; Trachenko, K. *J. Phys.: Condens. Matter* **2005**, *17*, S67–S75.

(49) Wakihara, T.; Kohara, S.; Sankar, G.; Saito, S.; Sanchez-Sanchez, M.; Overweg, A. R.; Fan, W.; Ogura, M.; Okubo, T. *Phys. Chem. Chem. Phys.* **2006**, *8*, 224–227.

(50) Keen, D. A. *J. Appl. Crystallogr.* **2001**, *34*, 172–177.

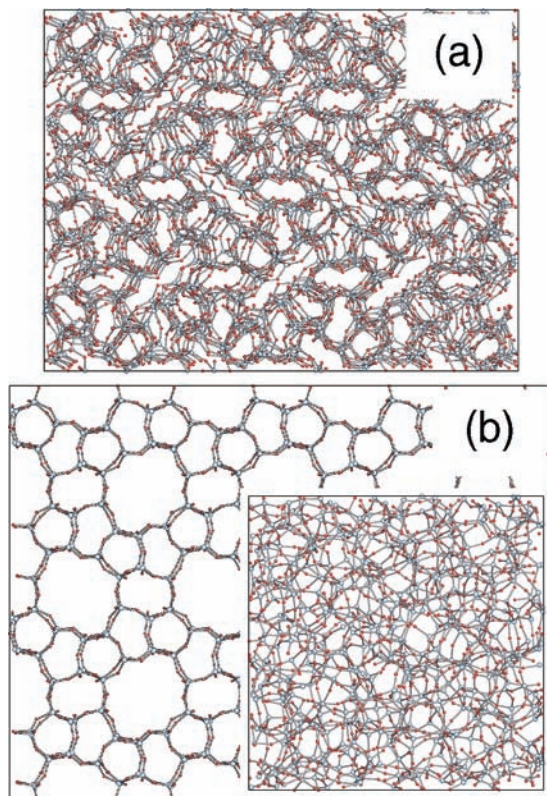


Figure 4. RMC models of pressure amorphized silicalite-1-F (a) and silica glass⁴⁸ (inset to (b)) and the structure of silicalite-1-F projected along the [010] direction (b) (to scale, note that there are less atoms in the model for silica glass).

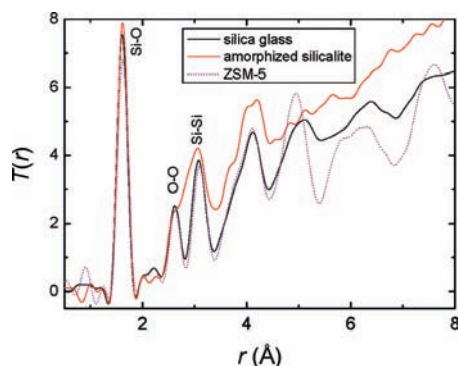


Figure 5. Total correlation functions $T(r)$ of pressure-amorphized silicalite, silica glass and an amorphous precursor used to prepare the zeolite ZSM-5.⁴⁹ $T(r)$ have been obtained by direct Fourier transformation of the total X-ray structure factor, $S(Q)$.⁵⁰

the structure of pressure-amorphized silicalite-1-F, being very different from those of normal and densified silica glass and of the amorphous precursor used to prepare the silica-rich zeolite ZSM-5, is indeed a novel form of amorphous silica.

The pressure-amorphized material ($\rho = 2.7 \text{ g/cm}^3$) is 51% more dense than silicalite-1-F ($\rho = 1.787 \text{ g/cm}^3$) and 23% more dense than silica glass ($\rho = 2.2 \text{ g/cm}^3$). The density of the pressure-amorphized material *in situ* at 20 GPa may be expected to be of the order of 3.5 g/cm^3 based on the study of silica glass.¹³ Such a density value would be consistent with 4-fold coordinated silicon and a structure exhibiting the same basic framework as the recovered pressure-amorphized material. It is clear that the amorphization (and attendant loss of periodicity) is linked to the collapse of the pores in the silicalite structure,

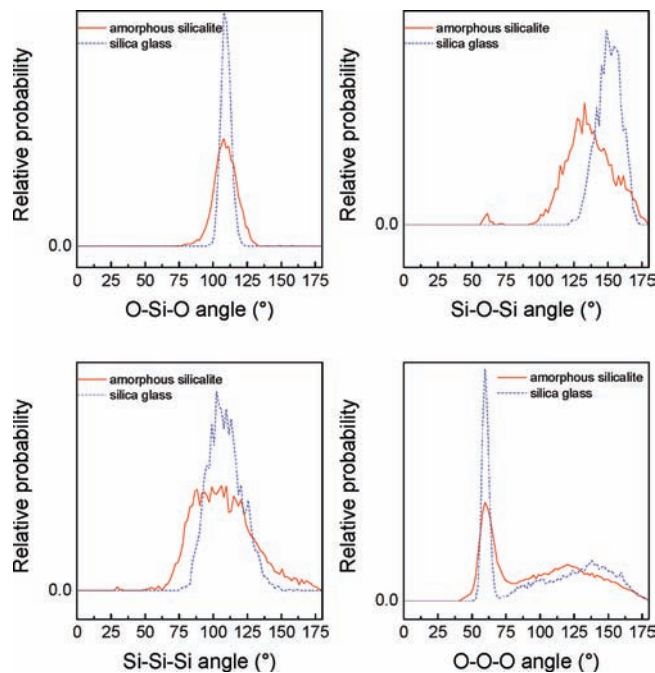


Figure 6. Bond angle distributions from the RMC model of pressure-amorphized silicalite-1-F and silica glass.⁴⁸

which occurs through large random local changes in Si–O–Si bond angles based on the strong broadening of the Si–Si correlation (see Figure 5). The strong reduction in Si–Si–Si and Si–O–Si bond angles with respect to silica glass (see Figure 6) and the presence of a double peak in the Si–Si correlation (Figure 3B) are indicative of highly strained configurations on different length scales, respectively; in the ring edges and locally in the Si–O–Si angles around the oxygen atoms. This intertetrahedral Si–O–Si angle distribution in amorphized silicalite-1-F is centered around 125° rather than $145\text{--}150^\circ$ and is much broader than in silica glass (see Figure 6).

There are small voids corresponding in particular to the collapsed 5, 6, and 10 MRs of the initial crystalline structure. The present experimental results and RMC model indicate that the amorphization can take place while still retaining remnant periodicity and without a major change in ring statistics. The ring statistics in pressure-amorphized silicalite-1-F found in Figure 4 can be explained by an extraordinary “topologically ordered” structure (i.e., still retaining the initial chemical bonds and connectivity); amorphous materials usually exhibit “topologically disordered” structures^{51,52} in which ring statistics are very broad and very different from the corresponding crystal phase.⁵³ Inspection of the silica glass model (Figure 4, inset) shows that voids are also present, but distributed in a random manner, more a characteristic of a quenched liquid.

The amorphous structure can helpfully be compared with the pressure-induced amorphous structures produced at high pres-

(51) Cooper, A. R. *Phys. Chem. Glasses* **1978**, *19*, 60–68.

(52) Gupta, P. K.; Cooper, A. R. *J. Non-Cryst. Solids* **1990**, *123*, 14–21.

(53) Amorphous materials usually exhibit topologically disordered structure according to Cooper and Gupta. For example, silica glass has a very broad ring statistics from 3 to 10 MRs centered at 6 MR,^{54,55} whereas β -cristobalite has only 6 MR.

(54) Rino, J. P.; Ebbsjö, I.; Kalia, R. K.; Nakano, A.; Vashishta, P. *Phys. Rev. B* **1993**, *47*, 3053–3062.

(55) Kohara, S.; Suzuya, K. *J. Phys.: Condens. Matter* **2004**, *17*, S77–S86.

tures using *ab initio* methods on zeolite structures.²⁷ In this study, a series of different structural motifs were obtained with increasing pressure which correspond to increased distortion of the zeolitic ring and pore structure with eventual collapse and increased bonding at the highest pressures. The pressure amorphized silicalite-1-F structure shown in Figure 4 is strongly reminiscent of the collapsed ring structures of the *ab initio* study at intermediate pressures. Interestingly, the *ab initio* structures at these pressures also do not involve bond breaking and show reduced average Si–O–Si bond angles.

Finally, a recent PDF study³⁰ of the pressure-amorphized, hydrated aluminosilicate zeolite Na-A indicates little change in the local environments around T (Al, Si) and Na atoms upon PIA. This is consistent with no measurable T–O bond breakage, which is in agreement with the present results concerning Si–O bonding. Major changes were, however, observed in correlations at longer distances linked to the specific secondary building units, such as sodalite cages and double 4 MRs, of the Na-A structure.

Conclusion

The present study emphasizes the difference between the vibrational properties and the structural topology of amorphous materials obtained by temperature-induced vitrification and those obtained by PIA of an open-structured, microporous, crystalline

material; the latter retains the basic topology of the initial crystalline phase, but with strong geometrical distortions. This opens the route to prepare new topologically ordered (i.e., still retaining the initial chemical bonds and connectivity), amorphous materials with different intermediate-range structures, a lower entropy with respect to a standard glass, distinct physical and mechanical properties, eventually approaching those of an “ordered” or “perfect” glass. The conservation of the topological order in analogous, but more complex, aluminosilicate zeolites will, in addition, also conserve the chemical order of the crystal in the amorphous material. The structural collapse, in particular around the empty pores, which is shown to occur in PIA of silicalite-1-F and leads to a high degree of densification, provides a mechanism for shock wave absorption in this material.

Acknowledgment. We would like to thank D. Bourgoigne of the ICGM for technical assistance and A. L. Goodwin for useful discussions. The synchrotron radiation experiments were performed at the BL04B2 in the SPring-8 with the approval of the Japan Synchrotron Radiation Research Institute (JASRI) (Proposal Number 2008A1965). The multianvil apparatus of the Laboratoire Magmas et Volcans is financially supported by the Centre National de la Recherche Scientifique (Instrument National de l'INSU).

JA904054V